JOURNAL OF SOLID STATE CHEMISTRY 88, 104–114 (1990)

Magnetic and Transport Properties of Magnetite in the Vicinity of the Verwey Transition

Z. KAKOL[1]

Department of Chemistry, Purdue University, West Lafayette, Indiana 47907

Received March 19, 1990

DEDICATED TO J. M. HONIG ON THE OCCASION OF HIS 65TH BIRTHDAY

Systematic investigations concerning the variation of the Verwey phase transition in magnetite $Fe_{3(1-\delta)}O_4$ on the metal-to-oxygen ratio by electrical resistivity, Seebeck coefficient, and magnetization measurements are reported, together with electrical properties of $Fe_{3-x}Zn_xO_4$ zinc ferrites. In conformity with earlier heat capacity measurements it has been documented that the transition temperature is significantly reduced with increasing δ. In the range $0 < \delta < \delta_c = 0.0039$ the transition is of first order, whereas for $\delta_c < \delta \leq 0.012$ it is of second (or higher) order. The electrical properties and Verwey transition of $Fe_{3-x}Zn_xO_4$ and $Fe_{3(1-\delta)}O_4$ were found to match very well with the compositional correspondence $x \Leftrightarrow 3\delta$. Implications of the above findings are discussed. © 1990 Academic Press, Inc.

1. Introduction

The low temperature transition of Fe_3O_4, termed the Verwey transition, is a transformation that has long been investigated but is still not completely understood.

The existence of low temperature transition in magnetite was documented in 1929 when Millar (*1*) reported a peak in specific heat curve at the transition temperature (cf. Fig. 1) and when Weiss and Forrer (*2*) found that the material is much harder to magnetize to saturation below this transition temperature. Also the electrical conductivity was found to decrease abruptly by a factor of about 100 (*3*). In 1939 Verwey (*4*) reported the electrical transition in Fe_3O_4 near 120 K that now bears his name. He proposed that below the transition temperature T_V the distribution of Fe^{2+} and Fe^{3+} ions in octahedral sites changes from dynamic disorder to long range order; he proposed that Fe^{2+} and Fe^{3+} layers laminate alternately along the *c*-axis. This ordered structure was thought to be orthorhombic, whose *c*-axis coincides with one of the cube edges and whose *a*- and *b*-axes lie along the orthogonal face diagonals. This particular investigation greatly increased interest in the magnetite system, and the nature of this transition has subsequently been the subject of an enormous number of investigations which continue to the present time. Because Fe_3O_4 is a prototype compound of the ferrites, even greater importance was attached to investigations of this class of materials since ferrites have found applications in industry as memory cores, high frequency

---

[1] On leave from the Department of Solid State Physics, Akademia Górniczo—Hutnicza, PL-30-059 Kraków, Poland.

0022-4596/90 $3.00

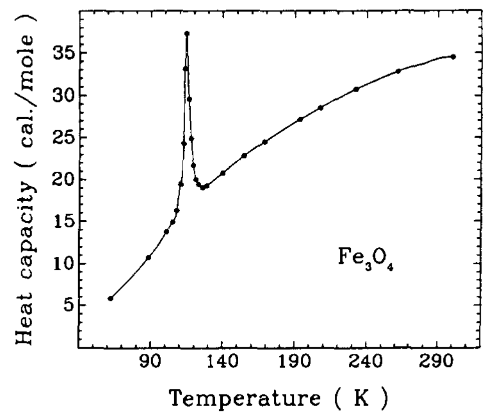

FIG. 1. The molar heat capacity of Fe_3O_4 (*1*).

communications materials, and magnetic materials for recording media. Despite the intense level of research involving many different aspects of the Verwey transition, as reflected in extensive literature that has been accumulated over a period of 50 years, there is no consensus with respect to the experimental results or theoretical interpretation of this phenomenon. Particularly, widely discordant results have been reported concerning heat capacity measurements, which is one of the basic techniques for investigating the Verwey transition. Westrum and collaborators (*5–8*) and Rigo and co-workers (*9–11*) had reported the existence of two closely spaced heat capacity peaks in the temperature range 100 to 125 K. This width of the transition ranged from 2 to 11 K. By contrast no such effect was found in early investigations (*1, 3*) on natural crystals and in later, carefully repeated measurements (*12, 13*) on synthetic single crystals and ceramics. It was clearly demonstrated that in pure, stoichiometric magnetite only a single sharp transition occurs. Close examination of the experimental data leads to the conclusion that many of the discrepancies in the literature may be traced to differences in sample preparation rather than attributed to faulty measurement techniques. It is well known that properties of many oxides depend critically on the oxygen stoichiometry. For example, the metal-insulator transition in V_2O_3 varies from approximately 14 to 180 K as the oxygen content is changed (*14*). Recent investigations of high-T_c superconductors show that the superconducting transition temperature T_c is very sensitive to oxygen stoichiometry; in $YBa_2Cu_3O_{7-\delta}$ compounds T_c decreases monotonically with oxygen vacancy concentration δ, reaching finally the point at which superconductivity is completely suppressed (*15*).

Verwey and Haayman (*16*) had already reported that an increase in the oxygen content of the Fe_3O_4 phase shifted the transition temperature from 120 to 100 K and that the jump in the resistance at the transition decreases as shown in Fig. 2. The transition disappears altogether for a sufficiently large oxygen excess. Later measurements of the heat capacity on undoped Fe_3O_4 led to the conclusion that cation vacancies play a dominant role in lowering T_v and in broadening transition (*17*). It is then clearly evident that oxygen stoichiometry control is at least as important as high purity and homogeneity of the sample.

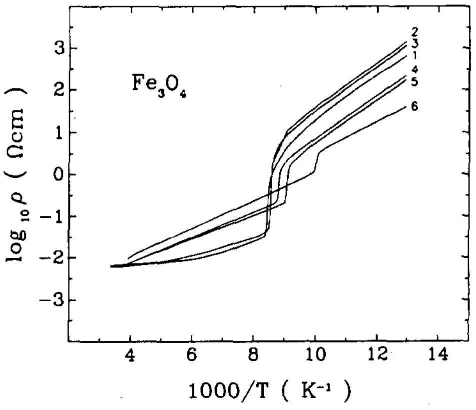

FIG. 2. Variation of resistivity (ρ) with temperature in magnetite (1) and in the same oxide with varying but small amounts of iron deficit (2–6) (*16*).

The first systematic investigations of the dependence of the Verwey transition in magnetite on the metal-to-oxygen ratio were reported recently. The heat capacity measurements (*18–21*) were performed on $Fe_{3(1-\delta)}O_4$ single crystals grown by the skull melting technique (*22*) and reannealed under a buffered CO–CO_2 atmosphere (*23*) using an oxygen transfer cell (*24*) to monitor the oxygen fugacity. The length of the anneals and the requisite oxygen fugacities were determined through the work of Dieckmann and co-workers, who have carried out a series of detailed studies on the cation diffusion to resolve the defects structure in magnetite (*25–31*). They determined the deviation δ from the stoichiometry in high temperature equilibrium state as a function of temperature and oxygen partial pressure.

In conformity with earlier published results the transition temperature was found to be a maximum for pure stoichiometric Fe_3O_4 and to decrease from 120 K to about 81 K with increasing departure from stoichiometric composition. The full circles in Fig. 15 show the variation of T_v with fractional cation vacancy δ as determined from heat capacity data, in a plot of T_v vs 3δ. Additionally, a previously unreported, fundamental phenomenon was discovered, namely that the Verwey transition is of first order in the composition range $-0.0005 \leq \delta \leq \delta_c$, $\delta_c = 0.0039$ and of second (or higher) order for $\delta_c < \delta \leq 3\delta_c$. The value $\delta_c = 0.0039$ corresponds to the critical value at which one of the 32 ferrous ions per (doubled) unit cell of the magnetite low temperature phase has been converted to a ferric ion as a result of the oxidation process. Representative heat capacity data for magnetite samples with $\delta \cong 0$ and $\delta = 0.0049$ are shown in Fig. 3. These data demonstrate that the Verwey transition represents a well-defined phase transformation in a thermodynamic sense.

In the present paper we review the electrical and magnetic properties of magnetite, emphasizing the dependence of these properties on the stoichiometry parameter δ. Also, recent results on the influence of Zn doping on Verwey transition are provided.

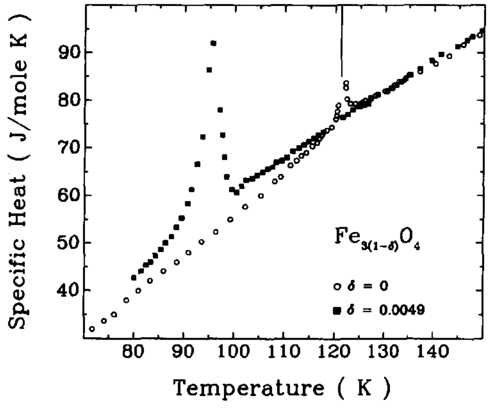

FIG. 3. Heat capacity of $Fe_{3(1-\delta)}O_4$ samples as a function of temperature (*20*). (○) $\delta = 0$; (■) $\delta = 0.0049$.

2. Background Information

Above the Verwey transition magnetite is in the cubic inverse spinel $(Fe^{3+})[Fe^{3+}, Fe^{2+}]O_4$ configuration (*32*) i.e., tetrahedral sublattice is occupied exclusively by Fe^{3+} ions whereas both Fe^{2+} and Fe^{3+} ions are present in octahedral sites. Above T_v magnetite has its magnetic hard, intermediate, and easy axes along the cubic $\langle 001 \rangle$, $\langle 110 \rangle$, and $\langle 111 \rangle$ directions, respectively (*33*). Two octans of the spinel structure are shown in Fig. 4. The crystal structure below the transition point was initially believed to be orthorhombic (*32, 34*); however, more recent experiments, i.e., neutron diffraction (*35*) and electron diffraction (*36*) suggested a monoclinic symmetry, with magnetic hard, intermediate, and easy axes coinciding respectively with the monoclinic *a* (cubic $[1\bar{1}0]$), *b* (cubic [110]), and *c* (cubic [001]) directions. The monoclinic *c*-axis is actually tilted ~0.20° away from the vertical toward the $-a$ direction due to a rhombohedral elongation along the $[\bar{1}11]$ or $[\bar{1}1\bar{1}]$ axes (*37*),

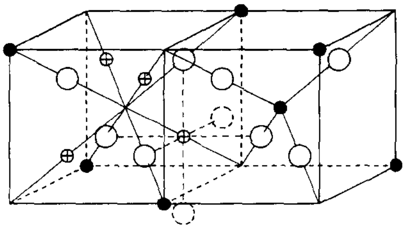

FIG. 4. Two octans of the spinel structure. The large spheres represent the oxygen ions. The small black and crossed spheres represent the iron ions on tetrahedral and octahedral sites, respectively.

TABLE I

THE COMPARISON OF TRANSITION TEMPERATURE T_v WITH THE CORRESPONDING RESISTIVITY CHANGE $\Delta \log \rho$ AT THE TRANSITION

125	2.4	(*37*)
122	2.1	(*40*)
121	2.1	(*41*)
120	2.1	(*16, 42*)
119	1.9	(*43*)
113	1.7	(*44*)
109	1.5	(*38*)
109	1.5	(*45*)

which results in twinning of the crystals (*37–39*). The role of twinning is important in the measurements and interpretation of electric and magnetic data. Relationship between the monoclinic unit cell and the rhombohedrally distorted cell is presented in Fig. 5.

3. Electrical Transport Properties

3.1 Experimental

The temperature dependence of the resistivity for nearly stoichiometric magnetite was measured by many authors who reported abrupt changes in resistivity of roughly two orders of magnitude in the temperature range 109 to 125 K. Some of the results are presented in Table I as a comparison of transition temperature T_v and the corresponding resistivity change $\Delta \log \rho$ at the transition. The noticeable trend, namely that the lower transition temperature is accompanied by a smaller change in resistivity, suggests according to results of Verwey and Haayman (*16*), Kuipers and Brabers (*46*), and Gillot and Jemmali (*44*) a departure from stoichiometry in samples with low T_v values. This tendency was strongly confirmed in recent systematic investigations of the electrical properties of magnetite as a function of metal-to-oxygen stoichiometry (*40, 47*). The electrical resistivity results for $Fe_{3(1-\delta)}O_4$ single crystal specimens within the composition range $-0.0006 < \delta < 0.010$ are presented in Fig. 6, as a plot of $\log \rho$ against inverse temperature. In agreement with heat capacity data (*19*) the transition temperature was found to be a strong function of δ. The change in the nature of the transition is also clearly evident. The first order transition is accompanied by a sharp discontinuity in electrical resistivity for $\delta < \delta_c$; only a change in slope is seen for samples with $\delta > \delta_c$ and this is accompanied by thermal hysteresis. Since thermal hysteresis cannot be associated

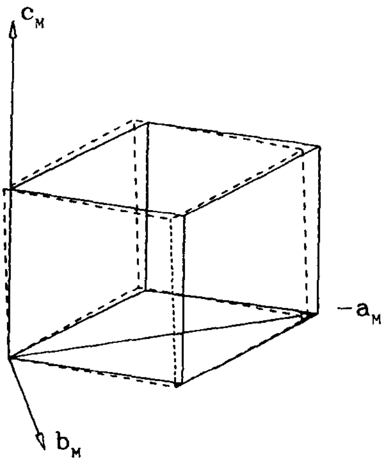

FIG. 5. Relationship between the monoclinic unit cell (a_M, b_M, c_M) and the rhombohedrally distorted cell (solid lines). The cubic unit cell is dashed.

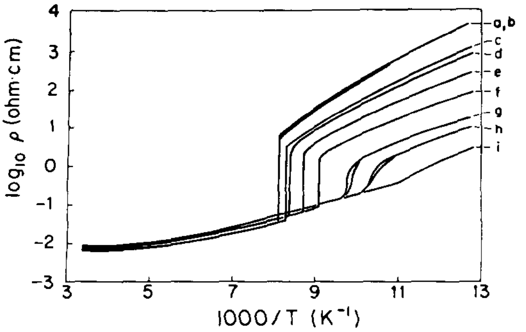

FIG. 6. Variation of resistivity (ρ) with temperature in magnetite $Fe_{3(1-\delta)}O_4$ for various δ values (*40*). (a) $\delta = -0.00053$; (b) $\delta = -0.00017$; (c) $\delta = 0.00021$; (d) $\delta = 0.00035$; (e) $\delta = 0.0017$; (f) $\delta = 0.0035$; (g) $\delta = 0.0050$; (h) $\delta = 0.0068$; (i) $\delta = 0.0097$.

with a second order transition and similar behavior is not observed in other physical properties, the possible existence of a nonohmic contribution to ρ was suggested (*40*).

The temperature dependence of the Seebeck coefficient (α) presented in Fig. 7 leads to similar conclusions. The transition is characterized by a decrease of α below T_v, which is discontinuous for $\delta < \delta_c$ and gradual for $\delta > \delta_c$. T_v is shifted to lower temperatures with rising δ. The introduction of nonstoichiometry defects in magnetite involves, during the annealing, the placement of oxygen at regular anion lattice sites of the crystal, followed by cation migration. In $Fe_{3(1-\delta)}O_4 \equiv (Fe^{3+})[Fe^{3+}_{1+6\delta}, Fe^{2+}_{1-9\delta}]O_4$; 6δ additional Fe^{3+} ions and 9δ fewer Fe^{2+} ions exist per formula unit than in Fe_3O_4. Thus, 3δ holes have been generated through the change in Fe^{2+}/Fe^{3+} ratio on the octahedral sites. The same change in carrier density may be introduced in magnetite by substitution of Zn^{2+} for Fe^{3+}. Zinc enters the tetrahedral sites exclusively, thereby introducing one hole per zinc ion on the octahedral site, on the generally accepted assumption that the remaining iron in the tetrahedral sublattice remains in the trivalent state. It is therefore of interest to investigate the changes in the Verwey transition that arise from Zn substitution.

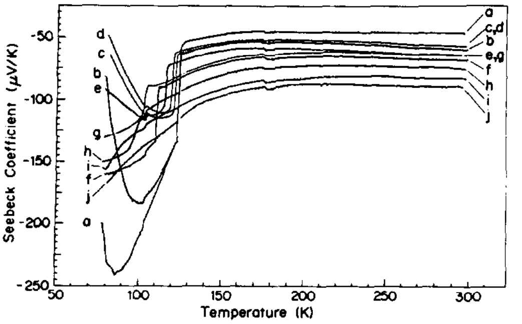

FIG. 7. Variation of Seebeck coefficient (α) with temperature in magnetite $Fe_{3(1-\delta)}O_4$ for various δ values (*40*). (a,b) $\delta = 0$; (c) $\delta = 0.00021$; (d) $\delta = 0.00069$; (e) $\delta = 0.0018$; (f) $\delta = 0.0036$; (g) $\delta = 0.0052$; (h) $\delta = 0.0070$; (i) $\delta = 0.0099$; (j) $\delta = 0.012$.

Recently, systematic investigations of the electrical properties of the single crystal zinc ferrites $Fe_{3-x}Zn_xO_4$ were reported (*48*). Electrical resistivity data for $Fe_{3-x}Zn_xO_4$ single crystals in the composition range $0 \leq x \leq 0.04$ are presented in Fig. 8 as a plot of log ρ vs inverse temperature. All of the crystals used in measurements were rendered stoichiometric (i.e., with a 4/3 oxygen-to-cation ratio) by appropriate subsolidus annealing (*49*). The transition for samples with $0 \leq x \leq 0.011$ is marked by a sharp discontinuity in ρ which decreases in magnitude and moves toward lower temperatures with increasing x. As in undoped magnetite this is taken to reflect the occurrence of a first order Verwey transition of T_v. Samples with $0.014 \leq x \leq 0.035$ exhibit an inflection point in the log ρ vs $1/T$ dependence, as indicated by the arrows in Fig. 8, identical with the inflection encountered in plots of ρ vs T. This is taken to reflect the occurrence of a second (or higher) order Verwey transition in the above range of composition. The change of the Verwey transition temperature T_v with x is compared with the T_v vs 3δ dependence for nonstoichiometric magnetite in Fig. 15. The obvi-

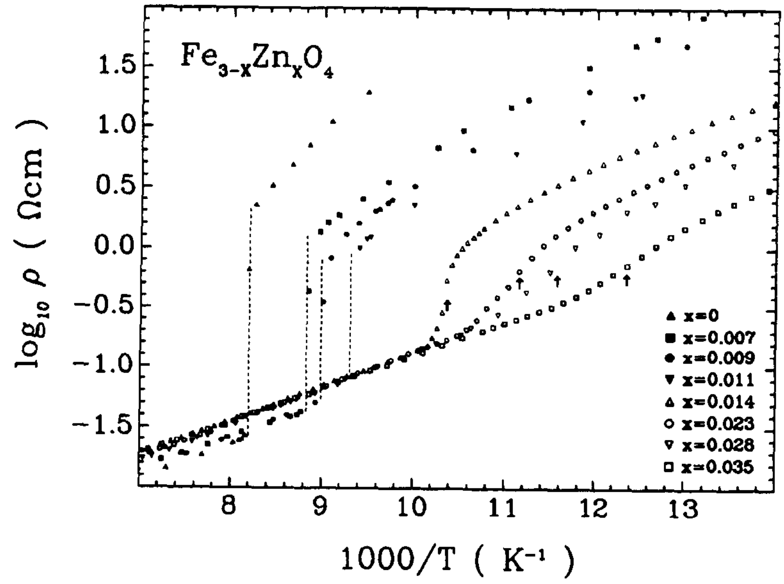

FIG. 8. Variation of resistivity (ρ) with temperature in zinc ferrites $Fe_{3-x}Zn_xO_4$ for various x values (*48*).

ous correspondence $x \Leftrightarrow 3\delta$ is very striking. A similar correspondence is apparent in Fig. 9 where plots of the resistivity discontinuity at the transition vs x and 3δ are presented. A further verification of the $x \Leftrightarrow 3\delta$ correspondence was obtained from a comparison of the Seebeck coefficients measured for zinc ferrites and nonstoichiometric magnetite (*48*).

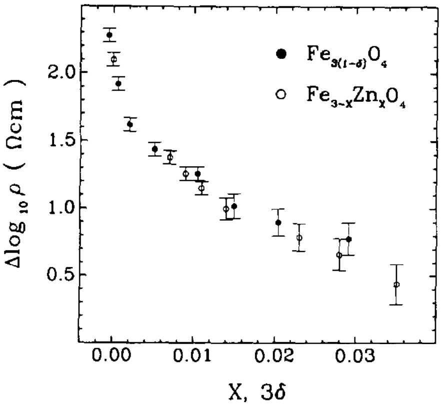

FIG. 9. Variation of the resistivity change $\Delta\rho$ at the transition in nonstoichiometric magnetite $Fe_{3(1-\delta)}O_4$ and in zinc ferrites $Fe_{3-x}Zn_xO_4$ with 3δ and x respectively (*48*).

3.2 Discussion

The results of the electrical resistivity and Seebeck coefficient measurements for $Fe_{3(1-\delta)}O_4$ single crystals indicate that even small departures from the ideal 4/3 oxygen-to-cation ratio strongly influence the Verwey transition.

The electrical properties and the Verwey transition for zinc ferrite single crystals $Fe_{3-x}Zn_xO_4$ match very well the data for nonstoichiometric magnetite $Fe_{3(1-\delta)}O_4$ with the compositional correspondence $x \Leftrightarrow 3\delta$. This correspondence for Seebeck coefficients points to an equivalence in charge carrier densities since the Seebeck coefficient in the nearly localized regime is directly related to the Fermi level, which in turn is determined by the charge carrier density. Furthermore the close match of the resistivity data subject to the correspondence $x \Leftrightarrow 3\delta$ indicates that not only the charge carrier densities but also the mobilities of the holes in the zinc ferrites and nonstoichiometric magnetites must be comparable. These findings suggest that conduction occurs by charge transport involving valence fluctuation on the cations in octahedral sublattice and that any cations vacancies present at these sites do not greatly impede the transport process.

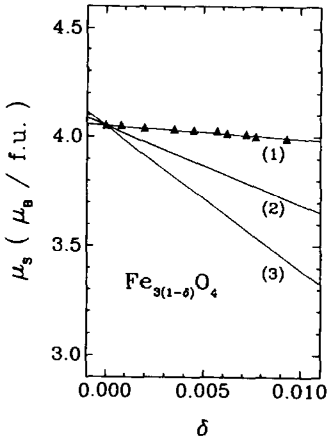

FIG. 10. Saturation moment (μ_s) of $Fe_{3(1-\delta)}O_4$ vs nonstoichiometry δ at 4.2 K *(56)*. (▲) Experimental data; lines (1), (2), and (3) represent calculated values (explanation in the text).

4. Magnetic Properties

4.1 Experimental

There have been many investigations of the magnetic properties of magnetite; a listing of the more extensive studies is provided in Refs. *(37–39, 43, 50–53)*. Considerable interest was centered on how the magnetic properties of Fe_3O_4 are altered at the Verwey transition, where discontinuities or anomalies occur in other physical characteristics. Recently, systematic investigations of the influence of deviation from ideal stoichiometry on the magnetic properties of magnetites $Fe_{3(1-\delta)}O_4$ were reported *(54–56)*.

Because the oxidation process generates Fe^{3+} ions (as well as vacancies) at the expense of Fe^{2+} ions, the saturation moment μ_s is a function of δ. In Fig. 10 the variation of μ_s with δ is shown at 4.2 K. The three lines in Fig. 10 were calculated on the basis that additional Fe^{3+} ions were created (1) exclusively at the octahedral sites, (2) randomly on octahedral and tetrahedral sites, or (3) exclusively on tetrahedral sites. The experimental points fit extremaly well to model (1) as is physically reasonable. This is also in full agreement with data reported by Ramdani *et al.* *(57)*.

The magnetocrystalline anistropy parameters were determined for both cubic and monoclinic phases as a function of δ and of temperature from $M(H)$ magnetization curves either by fitting theoretical $M(H)$ curves to the experimental data or from the areas enclosed between $M(H)$ curves measured along different crystal directions. Below T_V measurements were performed after the sample had been cooled in a magnetic field at an angle of ~35° from [001] in the $(1\bar{1}0)$, or equivalently in the (111) plane. This procedure defines a unique easy axis along a specific [001] direction and also removes *a–b* type of twinning *(32, 52)*; however, the *a–a* type of twinning is not eliminated. Subsequently, samples were cooled in a magnetic field oriented along [001] and measurements carried out in the (010) plane; here both *a–b* and *a–a* twinning had to be taken into consideration. Finally, it was also necessary to take cognizance of axis switching. When the external magnetic field was rotated the easy axis of magnetization readily switched from one cube edge to another. This fact limits the fields that can be applied at any given temperature and for any particular specimen, and thus restricts the range of measurements of anisotropy parameters. The reader is referred to several key surveys *(43, 52, 53)* for further discussion of the axis switching process. In Fig. 11 the resulting

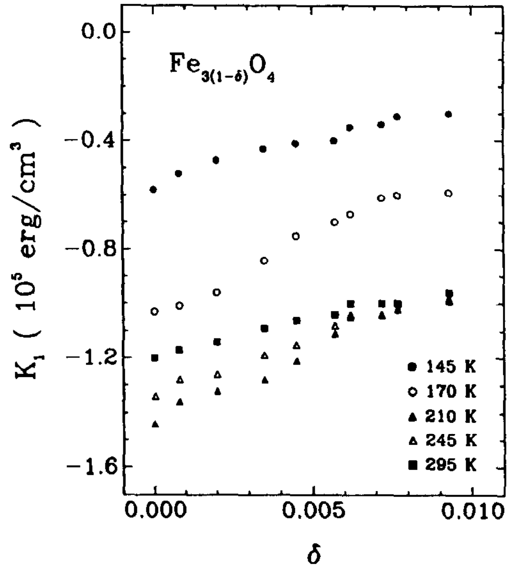

FIG. 11. Anisotropy parameter K_1 vs δ for $Fe_{3(1-\delta)}O_4$ in the temperature range 145–295 K (*56*).

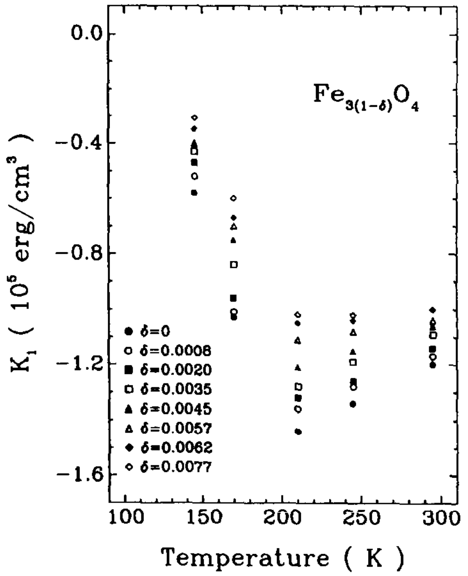

FIG. 12. Temperature dependence of K_1 anisotropy parameter for $Fe_{3(1-\delta)}O_4$ series (*56*).

K_1 cubic anisotropy parameter values are shown as a function of the stoichiometry parameter δ for several temperatures in the range 145 to 295 K. The temperature dependence of K_1 for variety of $Fe_{3(1-\delta)}O_4$ specimens is presented in Fig. 12. The anisotropy coefficient K_1 passes through minimum (maximum anisotropy field) and vanishes near 130 K for all δ. There is no discontinuity or other anomaly at critical value δ_c. The present results for stoichiometric magnetite are in good agreement with some earlier results based on both resonance measurements (*50*) and on magnetotorque studies (*58, 59*). The various calculated anisotropy constants for the low temperature phase of magnetites are shown in Fig. 13 as a plot of K vs δ at 4.2 K. The $\tilde{K}_a$ and $\tilde{K}_b$ are the orthorhombic anisotropy constants modified by the term added to deal with the rhombohedral distortion. For details see Refs. (*52, 53, 56*). The temperature dependence of the dominant anisotropy parameter $\tilde{K}_a$ is presented in Fig. 14. The insert shows the variation of the $\tilde{K}_b$ anisotropy parameter. The temperature range of measurements is increasingly narrowed with rising δ because of the progressively earlier onset of axis switching. The data on stoichiometric mag-

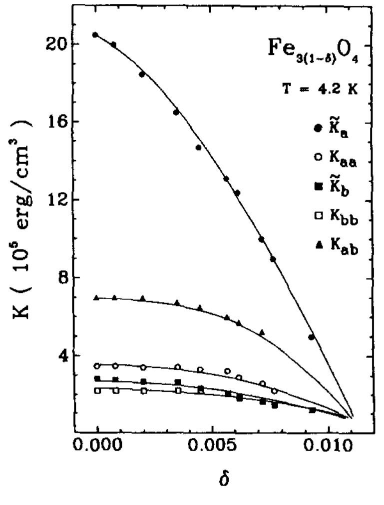

FIG. 13. Anisotropy parameters vs δ for $Fe_{3(1-\delta)}O_4$ at 4.2 K (*56*).

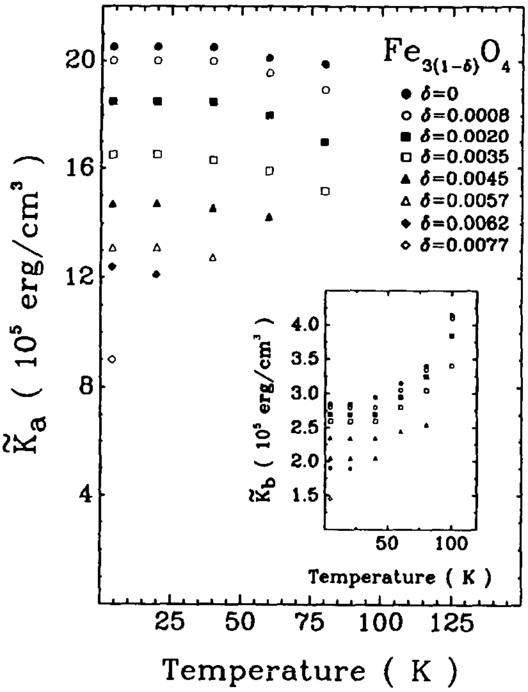

FIG. 14. Temperature dependence of anisotropy parameters $\tilde{K}_a$ and $\tilde{K}_b$ for $Fe_{3(1-\delta)}O_4$ series (*56*).

netite are in excellent agreement with earlier torque measurements by Palmer (*51*) and differ only slightly from data reported by Matsui and co-workers (*53*). One should note the strong decrease of $\tilde{K}_a$ with rising δ and the fact that other anisotropy parameters shown in Fig. 13 have nearly constant values up to at least 0.007. As $\delta \rightarrow 0.012$ all $K \rightarrow 0$. Note also, that $\tilde{K}_a$ values are not sensitive to temperature changes whereas $\tilde{K}_b$ rises with T. The last finding, according to Abe *et al.* (*52*), suggests some type of ordering of the ions in the octahedral sublattice below T_v. Finally it is worth noting that measurements of the temperature dependence of the magnetization may be employed for the precise determination of T_v (*55*). To prevent the axis switching phenomenon the magnetization studies were carried out in fields below 500 Oe. In these very low fields the magnetic moments obey the inequality $\mu_{[110]} < \mu_{[111]} < \mu_{[001]}$ below T_v, and are nearly equal above T_v. The sudden discontinuity in $\mu_{[110]}$ and $\mu_{[111]}$ at the Verwey transition permits an accurate determination of T_v to be made. The variation of T_v with 3δ as read off from the magnetization data is entered in Fig. 15 as a set of triangles. The agreement with the data originally reported on the basis of the heat capacity studies (*20*) is satisfactory.

4.2 *Discussion*

The above-presented results lead to several conclusions. None of the anisotropy parameters shows a shift or slope discontinuity at the critical value δ_c where the change in the order of the Verwey transition occurs. It is then difficult to reconcile this fact with any model in which the Verwey transition is driven primarily by magnetic interactions. This conclusion is reinforced by the fact that the saturation moment changes by less than 0.1% at T_v (*60*). All the anisotropy parameters at the temperature 4.2 K approach zero at the extrapolated value $\delta_m \cong 0.012 \cong 3\delta_c$ which also coincides with the highest value of δ for which a transition can still be de-

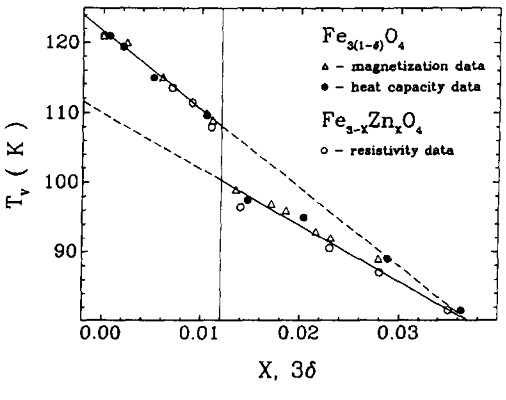

FIG. 15. Dependence of the Verwey transition temperature (T_v) on composition of zinc ferrites (x) or on oxygen stoichiometry of nonstoichiometric magnetite (3δ) (*48, 55, 61*).

tected (see Fig. 15). It was confirmed that T_v diminishes with rising δ, and that it exhibits a discontinuity near $\delta_c = 0.0039$.

5. Summary

It has been shown that the physical properties of magnetite depend critically on the stoichiometry parameter δ in $Fe_{3(1-\delta)}O_4$ where δ indicates the deviation of the oxygen-to-metal ratio from its ideal value of 4/3. By proper annealing of single crystals in appropriate oxygen fugacity it was possible to control systematically the dependence of electrical and magnetic properties on δ.

The principal conclusion to be drawn from above investigations is that the Verwey transition is of first order in the range $0 \leq \delta \leq \delta_c$ and of second (or higher) order for $\delta_c < \delta \leq 3\delta_c$ and no transition is found for $\delta \geq 3\delta_c$.

The electrical properties and the Verwey transition of zinc ferrites $Fe_{3-x}Zn_xO_4$ were found to match very well the data for nonstoichiometric magnetites $Fe_{3(1-\delta)}O_4$ with the compositional correspondence $x \Leftrightarrow 3\delta$. This finding suggests that charge transport occurs via valence fluctuations among iron ions on the octahedral sites and that any cation vacancies present at those sites do not greatly impede the transport process.

Measurements of the magnetic properties lead to the additional conclusion that the Verwey transition is not driven primarily by magnetic interactions.

Finally, the variation of the transition temperature T_v with δ, for nonstoichiometric magnetites, and with x, for zinc ferrites, are compared in Fig. 15 as a plot of T_v vs 3δ and x. These data serve as important experimental input data for the evaluation of several of the parameters in the very recent theoretical models dealing with interpretation of the Verwey transition (*61–64*). In these mean-field models the order parameter is introduced which represents the portion of frozen electrons in the ground state configuration.

Acknowledgments

Very stimulating discussions with J. M. Honig, J. Spałek, and J. W. Koenitzer are gratefully acknowledged. This research was supported by Grant NSF DMR 86—16533 A02.

References

1. R. W. Millar, *J. Amer. Chem. Soc.* **51,** 215 (1929).
2. P. Weiss and R. Forrer, *Ann. Phys.* **12,** 279 (1929).
3. F. Okamura, *Sci. Rep. Tohoku Univ. First Ser.* **21,** 231 (1932).
4. E. J. W. Verwey, *Nature (London)* **144,** 327 (1939).
5. B. J. Evans and E. F. Westrum, Jr., *Phys. Rev. B* **5,** 3791 (1972).
6. J. J. Bartel, E. F. Westrum, Jr., and J. L. Haas, Jr., *J. Chem. Thermodyn.* **8,** 575 (1976).
7. J. J. Bartel and E. F. Westrum, Jr., *J. Chem. Thermodyn.* **8,** 583 (1976).
8. G. B. Falk, L.-S. Pan, B. J. Evans, and E. F. Westrum, Jr., *J. Chem. Thermodyn.* **11,** 367 (1979).
9. M. O. Rigo, J. Kleinclauss, and A. J. Pointon, *Solid State Commun.* **28,** 1013 (1978).
10. M. O. Rigo and J. Kleinclauss, *Philos. Mag. B* **42,** 393 (1980).
11. M. O. Rigo, J. F. Marecle, and V. A. Brabers, *Philos. Mag. B* **48,** 421 (1983).
12. M. Matsui, S. Todo, and S. Chikazumi, *J. Phyas. Soc. Japan* **42,** 1517 (1977).
13. E. Gmelin, N. Lenge, and H. Kronmüller, *Philos. Mag. B* **50,** L41 (1984).
14. S. A. Shivashankar, Ph.D. thesis, Purdue University (1980).
15. P. Steiner, S. Hüfner, V. Kinsinger, I. Sander, B. Siegwart, H. Schmitt, R. Schultz, S. Junk, G. Schwitzgebel, A. Gold, C. Politis, H. P. Müller, R. Hoppe, S. Kemmler-Sack, and C. Kunz, *Z. Phys. B* **69,** 449 (1988).
16. E. J. W. Verwey and P. W. Haayman, *Physica (Utrecht)* **8,** 979 (1941).
17. E. Gmelin, N. Lenge, and H. Kronmüller, *Phys. Status Solidi* A **79,** 465 (1983).
18. J. P. Shepherd, J. W. Koenitzer, C. J. Sandberg, R. Aragón, and J. M. Honig, *Mol. Cryst. Liq. Cryst.* **107,** 191 (1984).
19. J. P. Shepherd, J. W. Koenitzer, R. Aragón, C. J. Sandberg, and J. M. Honig, *Phys. Rev. B* **31,** 1107 (1985).

20. R. Agarón, J. P. Shepherd, J. W. Koenitzer, D. J. Buttrey, R. J. Rasmussen, and J. M. Honig, *J. Appl. Phys.* **57**, 3221 (1985).
21. J. P. Shepherd, R. Aragón, J. W. Koenitzer, and J. M. Honig, *Phys. Rev. B* **32**, 1818 (1985).
22. H. R. Harrison and R. Aragón, *Mater. Res. Bull.* **13**, 1097 (1978).
23. R. Aragón, D. J. Buttrey, J. P. Shepherd, and J. M. Honig, *Phys. Rev. B* **31**, 430 (1985).
24. J. P. Shepherd and C. J. Sandberg, *Rev. Sci. Instrum.* **55**, 1696 (1984).
25. R. Dieckmann and H. Schmalzried, *Ber. Bunsenges. Phys. Chem.* **81**, 344 (1977).
26. R. Dieckmann and H. Schmalzried, *Ber. Bunsenges. Phys. Chem.* **81**, 414 (1977).
27. R. Dieckmann, T. O. Mason, J. D. Hodge, and H. Schmalzried, *Ber. Bunsenges. Phys. Chem.* **81**, 778 (1977).
28. R. Dieckmann, *Ber. Bunsenges. Phys. Chem.* **86**, 112 (1982).
29. R. Dieckmann C. A. Witt, and T. O. Mason, *Ber. Bunsenges. Phys. Chem.* **87**, 495 (1983).
30. R. Dieckmann and H. Schmalzried, *Ber. Bunsenges. Phys. Chem.* **90**, 564 (1986).
31. M. Backhaus-Ricoult and R. Dieckmann, *Ber. Bunsenges. Phys. Chem.* **90**, 690 (1986).
32. W. C. Hamilton, *Phys. Rev.* **110**, 1050 (1958).
33. L. R. Bickford, Jr., *Phys. Rev.* **76**, 137 (1949).
34. S. C. Abrahams and B. A. Calhoun, *Acta Crystallogr.* **8**, 257 (1955).
35. G. Shirane, S. Chikazumi, J. Akimitsu, K. Chiba, M. Matsui, and Y. Fujii, *J. Phys. Soc. Japan* **39**, 947 (1975).
36. T. Yamada, K. Suzuki, and S. Chikazumi, *Appl. Phys. Lett.* **13**, 172 (1968).
37. S. Chikazumi, *in* "Magnetism and Magnetic Materials (Philadelphia 1975), Proceedings of the 21st Annual Conference on Magnetism and Magnetic Materials, AIP Conf. Proc."
38. C. A. Domenicali, *Phys. Rev.* **78**, 458 (1950).
39. H. J. Williams, R. M. Bozorth, and A. Goertz, *Phys. Rev.* **91**, 1107 (1953).
40. R. Aragón, R. J. Rasmussen, J. P. Shepherd, J. W. Koenitzer, and J. M. Honig, *J. Magn. Magn. Mater.* **54–57**, 1335 (1986).
41. A. J. M. Kuipers and V. A. M. Brabers, *Phys. Rev. B* **20**, 594 (1979).
42. R. O. Zaitsev and V. A. Ivanov, *Sov. Phys. Solid State* **29**, 691 (1987).
43. B. A. Calhoun, *Phys. Rev.* **94**, 1577 (1954).
44. B. Gillot and F. Jemmali, *Phys. Status Solidi A* **77**, 339 (1983).
45. A. A. Samokhvalov and A. G. Rustanov, *Sov. Phys. Solid State* **7**, 961 (1965).
46. A. J. M. Kuipers and V. A. M. Brabers, *Phys. Rev. B* **14**, 1401 (1976).
47. R. J. Rasmussen, Ph.D. thesis, Purdue University (1988).
48. P. Wang, Z. Kakol, M. Wittenauer, and J. M. Honig, to be published.
49. P. Wang, Q. W. Choi, and J. M. Honig, *Z. Anorg. Allg. Chem.* **550**, 91 (1987).
50. L. R. Bickford, Jr., *Phys. Rev.* **78**, 449 (1950).
51. W. Palmer, *Phys. Rev.* **131**, 1057 (1963).
52. K. Abe, Y. Miamoto, and S. Chikazumi, *J. Phys. Soc. Japan* **41**, 1894 (1976).
53. M. Matsui, S. Todo, and S. Chikazumi, *J. Phys. Soc. Japan* **43**, 47 (1977).
54. Z. Kakol, R. N. Pribble, and J. M. Honig, *Solid State Commun.* **69**, 793 (1989).
55. Z. Kakol and J. M. Honig, *Solid State Commun.* **70**, 967 (1989).
56. Z. Kakol and J. M. Honig, *Phys. Rev. B* **40**, 9090 (1989).
57. A. Ramdani, T. Steinmetz, C. Gleitzer, J. M. D. Coey, and J. M. Friedt, *J. Phys. Chem. Solids* **48**, 217 (1987).
58. L. R. Bickford, Jr., J. M. Brownlow, and R. F. Penayer, *Proc. Inst. Electr. Eng., Part B* **104**, 238 (1957).
59. Y. Syono and Y. Ishikawa, *J. Phys. Soc. Japan* **18**, 1230 (1963).
60. S. Unemura and S. Iida, *J. Phys. Soc. Japan* **40**, 679 (1976).
61. R. Aragón and J. M. Honig, *Phys. Rev. B* **37**, 209 (1988).
62. J. M. Honig and R. Aragón, *Physica B/C* **150**, 129 (1988).
63. J. M. Honig, *Phys. Chem. Miner.* **15**, 476 (1988).
64. J. M. Honig and J. Spałek, *J. Less-Common Met.* **156**, 423 (1989).